ELSEVIER

Polymer 44 (2003) 1117–1131

polymer

www.elsevier.com/locate/polymer

# The hot compaction behaviour of woven oriented polypropylene fibres and tapes. I. Mechanical properties

P.J. Hine[a], I.M. Ward[a,*], N.D. Jordan[b], R. Olley[b], D.C. Bassett[b]

[a]*Department of Physics and Astronomy, IRC in Polymer Science and Technology, University of Leeds, Woodhouse Lane, Leeds LS2 9JT, UK*
[b]*Department of Physics, University of Reading, Reading RG6 4AF, UK*

Received 1 August 2002; received in revised form 22 October 2002; accepted 23 October 2002

## Abstract

The aim of this work was to establish the important parameters that control the hot compaction behaviour of woven oriented polypropylene. Five commercial woven cloths, based on four different polypropylene polymers, were selected so that the perceived important variables could be studied. These include the mechanical properties of the original oriented tapes or fibres, the geometry of the oriented reinforcement (fibres or tapes), the mechanical properties of the base polymer (which are crucially dependant on the molecular weight and morphology), and the weave style. The five cloths were chosen so as to explore the boundaries of these various parameters, i.e. low and high molecular weight: circular or rectangular reinforcement (fibres or tapes): low or high tape initial orientation: coarse or fine weave.

A vital aspect of this study was the realisation that hot compacted polypropylene could be envisaged as a composite, comprising an oriented ‘reinforcement’ bound together by a matrix phase, formed by melting and recrystallisation of the original oriented material. We have established the crucial importance of the properties of the melted and recrystallised matrix phase, especially the level of ductility, in controlling the properties of the hot compacted composite.

*Keywords:* Mechanical properties; Hot compaction behaviour; Polypropylene

## 1. Introduction

There are often applications for plastics which require enhanced performance, over and above that which can be achieved with an unfilled polymer. One widely used solution is to mix the base polymer with a stiffer reinforcement, in the form of straight, chopped or woven glass fibres. Although the resulting fibre reinforced composite has improved mechanical properties over the unfilled polymer, the density is increased and thermoformability and recyclability can be compromised. The issues of lightweight and recyclability are becoming increasingly important to the further exploitation of these materials in a number of industries, in particular the automotive sector.

An alternative strategy, which has formed the basis of research at Leeds, is to enhance the properties of the base polymers by the development of very high degrees of preferred molecular orientation [1,2]. In particular, solid phase deformation below the melting point has been found to be successful in developing very high degrees of molecular orientation in a range of semicrystalline polymers, including polyethylene [3], polypropylene [4] and polyoxymethylene [5]. By a suitable combination of initial morphology and solid phase processing conditions, highly oriented materials can be produced with stiffness and strength values at least an order of magnitude greater than the original isotropic polymers. High modulus polymer fibres can be combined with a suitable matrix to form a composite [6,7], but there are problems with this approach. When two different polymers are used there is the issue of recyclability, and there is also a problem in developing a good bond between the different polymers that comprise the fibre and matrix phases. There is, therefore, increasing interest in the area of polymer/polymer composites, as they offer the opportunity to bridge the performance gap between isotropic unfilled polymers and glass reinforced polymers, while offering possibilities for improved lightweight and recyclability over traditional composites. This is

---

[*] Corresponding author. Tel.: +44-113-3433808; fax: +44-113-3433809.

*E-mail address:* i.m.ward@leeds.ac.uk (I.M. Ward).

0032-3861/03/$ - see front matter © 2002 Published by Elsevier Science Ltd.
PII: S0032-3861(02)00809-1

particularly the case when the fibre and the matrix are both thermoplastic in nature.

A variety of different techniques have been reported in the literature for the production of single polymer composite materials: in the main this research has concentrated on unidirectional polyethylene (PE) fibre reinforced PE. Capiati and Porter [8] were first to use the term, one-polymer composite, in their work on a single high modulus PE filament embedded in a block of high density PE (HDPE). They measured high interfacial shear strengths in their model single fibre material and attributed this to the development of an epitaxial transcrystalline layer between the fibre and the matrix. Subsequent work by for instance Teishev et al. [9] and Marais and Feillard [10], extended this technique to making unidirectional PE/PE composites using film stacking. Other techniques explored have included powder impregnation [11] and solvent impregnation [12]. In all these processing methods, a major issue is compatibility between the fibre and matrix, which although a single polymer type, are usually of different molecular structure (e.g. HDPE and LDPE). Furthermore, wetting out of the fibre by the viscous thermoplastic 'matrix' can be a problem, unless a solvent route is used.

Although the majority of the published work on single polymer composites is concerned with polyethylene, the work of Loos et al. [13] explores polypropylene using a further different processing technique. Here, the approach is to use a bicomponent fibre, where an oriented fibre core is surrounded by a lower melting point material. On processing, the outer skin material is melted to form a matrix to bind the structure together. Wetting is no longer a problem in this case, as each fibre is surrounded by the requisite matrix phase, but compatibility can still be an issue.

Recent research at Leeds University has seen the development of an alternative manufacturing process for the production of polymer/polymer composites. The essence of this technique, termed hot compaction, is to take arrays of oriented fibres and tapes, and choose suitable conditions of temperature and pressure such that a thin skin of each fibre or tape is 'selectively' melted. On cooling, this molten material recrystallises to bind the whole structure together. The resulting hot compacted material is therefore composed of a single, and moreover, identical polymeric material, and by virtue of molecular continuity between the phases has excellent fibre/matrix adhesion. Also, by virtue of melting the skin of each fibre or tape, there is no matrix wetting problems.

Initial studies [14,15] investigated the hot compaction performance of unidirectionally arranged high modulus melt spun polyethylene fibres. A combination of mechanical testing and morphological studies was used to investigate the hot compaction mechanisms, and showed that selective surface melting did, in fact, occur for each fibre. The morphological studies [16] showed that, like the other published PE/PE work described above, excellent fibre to matrix adhesion was achieved through epitaxial crystallisation of the molten matrix onto the oriented fibres. An advantage of the hot compaction technique, over other processes, is that molecular continuity is achieved between the 'fibre' and 'matrix' phases.

Further work proceeded on unidirectional polyethylene terephthalate fibres [17], high modulus gel spun polyethylene fibres [18], and woven polypropylene tapes [19,20]. The compacted woven polypropylene results have proved valuable from a commercial standpoint, because the hot compacted sheets showed an interesting portfolio of properties including lightweight, good stiffness and strength and outstanding impact performance even at low temperatures [21]. Equally important, the hot compacted polypropylene sheets were found to be thermoformable [22].

Our previous studies were based on only a single polypropylene fabric. The present investigation is aimed at identifying key fabric parameters, which affect the properties of the final compacted sheet. The hot compaction behaviour of five commercially available woven cloths, based on four different polypropylene polymers has, therefore, been studied. The aim in choosing these materials was to explore the likely boundaries of the perceived important variables, which include the stiffness and strength of the oriented phase, the geometry of the oriented phase, the molecular weight and morphology of the base polymer and the weave style of the woven cloth. As in the previous hot compaction studies, a combination of mechanical testing techniques and morphological studies has been used to compare and contrast the compaction behaviour of each of the five chosen materials. This paper concentrates mainly on the mechanical aspects of the study and a companion paper describes the associated morphological studies

## 2. Experimental

### 2.1. Starting materials

Five woven oriented polypropylene cloths were obtained from commercial sources. Fig. 1 shows pictures of the five cloths all taken at the same magnification: the length of the bottom axis of each picture is 20 mm (scale shown on some of the pictures) and the bottom axis is parallel to the weft direction of each cloth. Table 1 shows the technical details of the five cloths, including fabric weight, weave style, count of tapes (per 10 cm) and a qualitative indication of the degree of crimp in the weft and warp directions. Table 2 gives details of the oriented polypropylene reinforcements and the base polymers used in the cloths. The polymers are numbered in order of increasing molecular weight (numbers 1–4).

*Cloth A*. This is a plain weave cloth composed of multifilament bundles. The fibres are produced from polymer 1, which has the lowest molecular weight. It also has the lowest density, but this could be due to the fact that it is

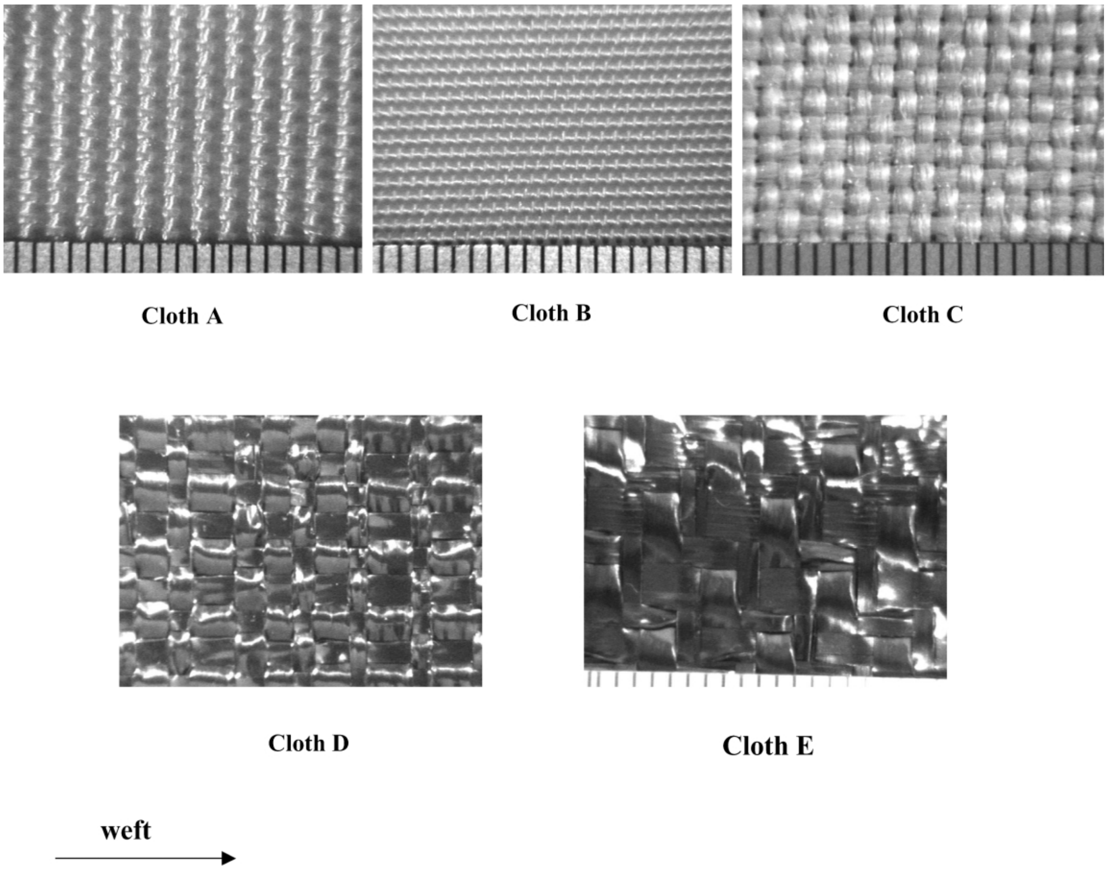

Fig. 1. Photographs of the five oriented polypropylene cloths used in this study: the bottom axis is 20 mm in all cases and parallel to the weft direction.

unpigmented, whereas the other three are coloured. The cloth has almost straight bundles of fibres in the warp direction, more closely spaced but more highly crimped fibre bundles in the weft direction. This configuration gives the cloth a ribbed appearance, with the ribs running parallel to the warp. As will be seen, this difference has implications for tensile modulus, tensile strength and peel strength.

*Cloth B*. This cloth is also composed of multifilament fibre bundles of polymer 1, but with a lower denier. As the picture in Fig. 1 shows, it is consequently a much tighter weave style. The cloth is reasonably balanced in the warp and weft direction, although the weft fibres have less crimp.

*Cloth C*. This is a plain weave fabric woven from fibrillated tapes. It is the second heaviest of the five fabrics studied, with an areal density of 294 g/m$^2$. The molecular weight of the base polymer for this cloth (polymer 2) is much higher than for polymer 1, in the mid range of those under study.

*Cloth D*. This is a plain weave fabric composed of flat tapes. The tapes are relatively thin, and so every other one is folded, presumably, to increase the areal density of the final cloth. Even so, the areal density is low at 136 g/m$^2$. The degree of crimp was not balanced in this cloth, with the weft tapes being much straighter compared to the warp tapes. The molecular weight of the base polymer is similar to polymer 2. Interestingly, the density of this tape is significantly

Table 1
Properties of the woven cloths

| Weave code | Oriented material | Polymer code | Fabric weight (g/m$^2$) | Weave style | Number of tapes/fibres (per 10 cm) | | Degree of crimp | |
|---|---|---|---|---|---|---|---|---|
| | | | | | Weft | Warp | Weft | Warp |
| A | Multifilament bundles | 1 | 297 | Plain | 90 | 60 | High | Low |
| B | Multifilament bundles | 1 | 236 | Plain | 140 | 140 | Medium | Medium |
| C | Fibrillated tape | 2 | 294 | Plain | 90 | 80 | Low | High |
| D | Flat tape | 3 | 136 | Plain | 60 | 60 | Low | High |
| E | Flat tape | 4 | 131 | Twill 2/2 | 60 | 60 | Low | Low |

Table 2
Properties of the oriented polypropylene reinforcements

| Polymer code | 1 | 2 | 3 | 4 |
|---|---|---|---|---|
| Reinforcement type | Multifilament bundles | Fibrillated tape | Flat tape | Flat tape |
| Young's modulus $E$ (GPa) | 9.5 | 10.9 | 6.2 | 6.8 |
| Failure strength $\sigma_F$ (MPa) | 453 | 350 | 370 | 422 |
| Failure strain $\varepsilon_F$ (%) | 12 | 6 | 16 | 16 |
| Density $\rho$ (kg/m$^3$) | 907 | 912 | 932 | 910 |
| $M_n$ | 38,500 | 55,800 | 56,100 | 78,100 |
| $M_w$ | 191,000 | 290,000 | 325,000 | 360,000 |
| Tape width (mm) | – | 1 | 2.5 | 2.5 |
| Tape thickness (mm) | – | 0.12 | 0.046 | 0.05 |
| Filament bundle diameter (mm) | 0.41 | – | – | – |
| Denier (g for 9000 m) | Cloth A: 1080<br>Cloth B: 450 | 1640 | 1030 | 990 |

$E$, $\sigma$, $\varepsilon$ $\pm 3\%$, $\rho \pm 0.1\%$, $M_w$, $M_n \pm 1\%$.

higher than the other reinforcements. This is most likely due to the presence of a heavier additive, as DSC measurements suggest a similar crystallinity to the other comparable materials.

*Cloth E.* This is a 2 × 2 twill cloth, composed of flat tapes of similar dimensions to cloth D. The base polymer for this cloth (polymer 4) has the highest molecular weight of the four. The degree of crimp in the warp and weft is balanced for this fabric.

## 2.2. Sample preparation

The preparation of the hot compacted sheets was carried out using a single pressure process as described previously in published work on woven polypropylene [19,20]. Firstly, the required number of woven layers was stacked in a matched metal mould (125 mm$^2$). In an improvement to the previous studies, a thermocouple was placed between the central two layers to allow the actual assembly temperature to be measured. The assembly was then placed into a hot press set at the required compaction temperature, and a pressure of 2.8 MPa (400 psi) was immediately applied. Once the assembly reached the compaction temperature, it was left for a further 10 min, at which time it was cooled to 100 °C and the sample was removed.

In order to measure the interlayer strengths developed during compaction, some samples were made using just two layers of cloth. For these samples a thin layer of aluminium foil, 10 mm wide, was placed at one end and between the layers to act as a starting crack on testing. With these thin two layer samples, it proved advantageous to place a rubber sheet inside the mould cavity to help even out the applied pressure. All the samples were laid up with the warp and weft fibres in the different layers aligned, normally termed a 0/0 layup.

In order to assess the mechanical properties of the matrix phase, melted films were made from the various cloths. These were produced by taking layers of the cloths to 200 °C, between copper plates, and after a short dwell time, cooling to room temperature. Various cooling rates were employed for these melted films.

## 2.3. Characterisation

### 2.3.1. Density

The densities of the original oriented materials, the compacted sheets and the melted films were measured using a density column. The column was made from a mixture of digycidyl ether and isopropanol to give a density range of ~890 to ~930 kg/m$^3$. While it is probably safe to compare the relative changes in density, and the likely changes in morphology and crystallinity, due to compaction and melting, it is perhaps unwise to attempt to calculate absolute values of crystallinity. This is so, because several of the oriented fibres and tapes contain proprietary pigments and additives which will obviously change the base density level.

### 2.3.2. Molecular weight

The molecular weight of the four base polymers was measured at RAPRA under the EPSRC scheme. Gel permeation chromatography was carried out on a Waters 150C, using 1,2 dichlorobenzene plus antioxidant at 140 °C and a flow rate of 1.0 ml/min. A refractive index detector was used.

### 2.3.3. DSC

The melting behaviour of the various materials was measured using a Perkin Elmer DSC7 differential scanning calorimeter at a scan rate of 10 °C/min. A comparison of the areas of the melting endotherms of the original oriented materials and the compacted sheets, allowed the percentage of melted material at each compaction temperature to be determined.

### 2.3.4. Mechanical properties

The stress/strain behaviour of the original oriented materials, the hot compacted sheets and the melted films was measured using an RDP Howden servo-mechanical tensile testing machine. The tensile tests on the compacted sheets and the melted films were carried out following ASTM D638 using a dumbbell shaped specimen. A nominal strain rate of $10^{-3}$ $s^{-1}$ was used for all the tests. The sample strain during the tests was measured using a Messphysik video extensometer.

Interlayer adhesion was measured using a T-Peel test (ASTM D1876). Samples, 10 mm wide and 100 mm long, were tested at a crosshead speed of 100 mm/min. T-peel tests were carried out parallel to both the weft and warp directions.

### 2.3.5. Fracture surfaces/morphology

Low magnification photographs of peel surfaces were taken through a Citoval stereomicroscope (Zeiss Jena). The peeled tapes were mounted loosely on matt black paper to minimise reflected light coming from below, and illuminated by two lamps at two perpendicular directions each at 45° from the peel direction and angled vertically about 35° from the horizontal, together with a roughly equal intensity of overhead illumination from the normal laboratory lighting. For higher magnification pictures of peel surfaces, these were coated with gold and examined under a Philips 515 Scanning Electron Microscope (SEM). Specimens were tilted 45° in order to improve contrast and give a good 3-dimensional impression.

## 3. Results

### 3.1. Properties of the oriented reinforcement

Fig. 2 shows stress–strain curves for the oriented reinforcements for each cloth (data in Table 2) at a nominal strain rate of $10^{-3}$ $s^{-1}$. All the drawn polypropylene materials showed similar tensile behaviour, with an initial linear region to ~0.8% (0.008) strain, followed by a region of continued strain hardening with a lower slope. The higher the initial modulus, which is predominantly determined by the degree of orientation, the higher the strain hardening rate, termed here the post-yield modulus. The failure strength increased with increasing initial modulus with the exception of the fibrillated tape made from polymer 2. The fibrillated nature of this material means that there is likely to be uneven stress transfer across the width of the tapes, leading to possible early failure. When these tapes are compacted, this is likely to be less important, and as will be seen later, these samples then showed a higher failure strength.

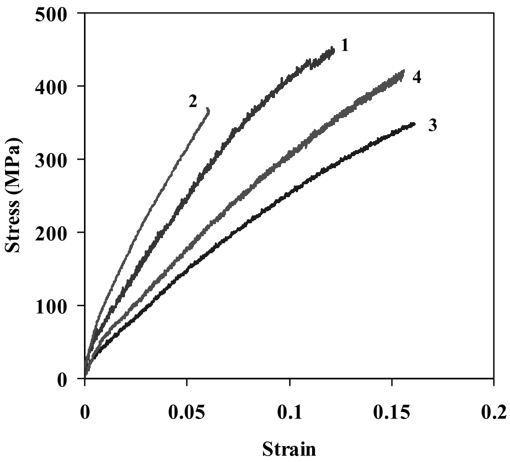

Fig. 2. The stress–strain curves of the original oriented materials.

### 3.2. Properties of the melted and recrystallised ('matrix') phase

To obtain an indication of the properties of the melted and recrystallised 'matrix' phase, films were made by melting out samples of the original woven cloths using a temperature of 200 °C. The key question was what cooling rate to use. Films were made using three cooling regimes: firstly, quenching into cold water; secondly, cooling at the same rate used when making hot compacted samples (~20 °C/min) and thirdly, slow cooling (~2 °C/min). It was hoped that the melted out samples, cooled at the same rate as the hot compacted samples, would most closely reflect the properties of the melted material in the hot compacted composites. The melted film samples were all tested at a strain rate of $10^{-3}$ $s^{-1}$.

Results are shown in Fig. 3, for the four polymer types. The results showed that for all four polymers, the quenched samples were ductile and drew in a stable manner with the formation of a stable neck region. Strain for these samples was measured from the crosshead speed, rather than directly on the sample, for if the neck formed outside the measurement region, the strain in the measurement region actually decreased.

First, we consider samples made using the intermediate (hot compacted) cooling regime (termed fast cool), where interesting differences in behaviour were seen. The lowest molecular weight polymer (number 1) showed an initial linear region, with an increased slope compared to the quenched sample, a yield point, again higher than the quenched sample, then rupture. This form of stress–strain behaviour is often termed necking-rupture [23,24]. The two intermediate molecular weight samples (numbers 2 and 3) showed stable drawing initially followed by rupture at ~25% strain. Only the highest molecular weight polymer (4) showed stable drawing, that is ductile behaviour, at this intermediate, fast cool, cooling rate.

All the samples made by slow cooling showed necking-rupture or brittle behaviour. In particular, the low molecular weight sample showed brittle failure at a low stress. In most cases the initial slope of the slow cooled samples was higher than either of the other two cooling rates, while the failure stress was between the fast cooled samples and the intermediate cooled sample. It is clear that the cooling rate of the hot compaction process is a key process parameter, because it has a significant effect on the mechanical properties of the matrix phase due to differences in morphology. Fast cooling

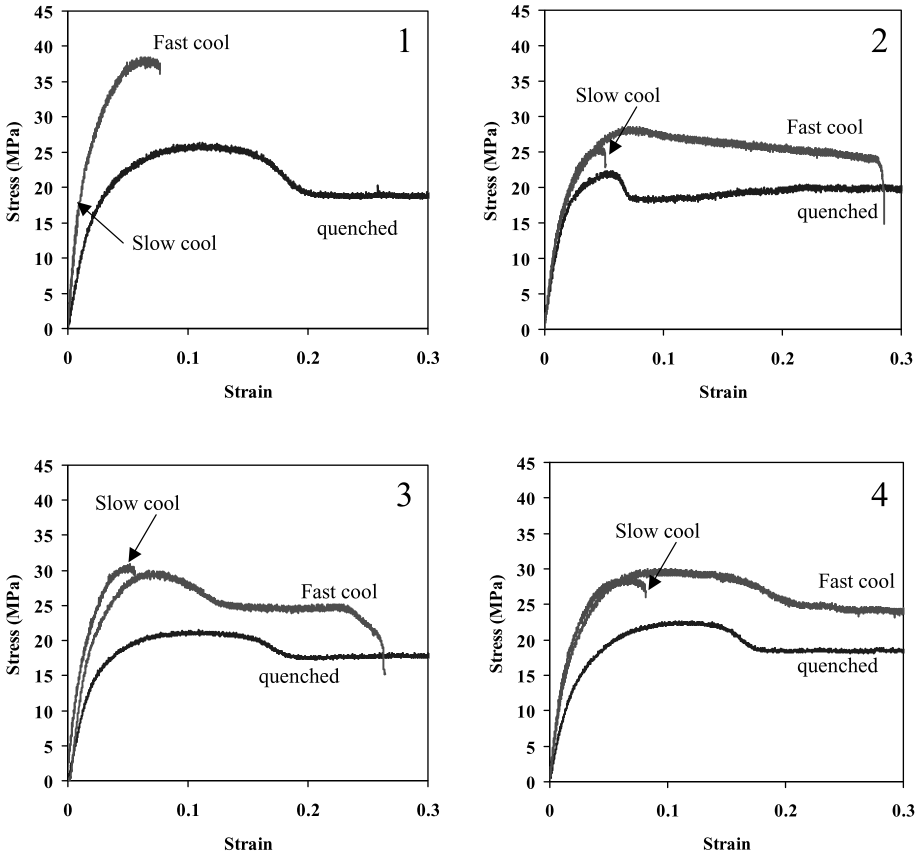

Fig. 3. The stress–strain curves of the melted films of the four polymers 1–4: quenched, fastest cooling rate on the press and slow cooled.

will produce lower crystallinity and more tie molecules leading to higher strengths, as proposed in polyethylene [25].

Table 3 shows the density and Table 4 shows the Young's modulus of the various melted films. The density of sample 3 is not given because it was too heavy for the density column, suggesting the incorporation of higher density additives for this polymer. Both the density and Young's modulus can be used as an indirect reflection of the crystallinity of the films, as we can attribute increases in either parameter with an increase in crystallinity. As the cooling rate is decreased, the density and Young's modulus for each polymer type increased, suggesting the expected increase in crystallinity (and associated reduction in ductility). Further the polymer with the lowest molecular weight (1) showed the highest values of Young's modulus and the polymer with the highest molecular weight (4) the lowest values. As described above, the absolute density values of each material could be altered by additives (e.g. polymer 3) so it would be unwise to use the density values to directly calculate crystallinity, however, the relative changes are consistent.

Two important differences between the matrix in the compacted sheets and that of the completely melted sheets are worth a mention: the melted material in the hot compacted composite crystallises epitaxially onto the oriented backbone—this is not the case in the completely melted samples: secondly the testing regime for the melted out samples was plane stress (thin samples), whereas the matrix

Table 3
Densities of the various materials for polymers 1, 2 and 4

| Polymer code | | Density (kg/m$^3$) |
|---|---|---|
| 1 | Original fibres | 907 |
| | Melted film: quenched | 911 |
| | Melted film: slow cool | 915 |
| 2 | Original fibres | 912 |
| | Melted film: quenched | 920 |
| | Melted film: slow cool | 924 |
| 4 | Original tape | 910 |
| | Melted film: quenched | 920 |
| | Melted film:slow cool | 925 |

Table 4
Young's moduli of the melted films

| Polymer code | Quenched | Fast cool hot press | Slow cool |
|---|---|---|---|
| 1 | 1.04 ± 0.02 | 1.85 ± 0.05 | 2.08 ± 0.13 |
| 2 | 1.00 ± 0.03 | 1.58 ± 0.06 | 1.71 ± 0.11 |
| 3 | 1.00 ± 0.09 | 1.24 ± 0.09 | 1.33 ± 0.01 |
| 4 | 0.95 ± 0.06 | 1.22 ± 0.10 | 1.37 ± 0.08 |

material in the composite is likely to be under plane strain conditions, which will further inhibit ductility.

### 3.3. Properties of the hot compacted sheets

#### 3.3.1. Stress–strain behaviour

The optimum compaction temperature was determined for the five cloths by producing samples over a range of compaction temperatures. Fig. 4 and Table 5 shows a typical series of results, in this case for samples of cloth C compacted over a range of temperatures from 179 up to 191 °C. The full set of results, shown in Table 5, show that as the compaction temperature was raised, the initial modulus and ultimate strength passed through a maximum and then decreased, while the peel strength increased monotonically. Fig. 4 shows typical stress–strain curves for selected samples from these experiments. It is seen that for the 179 °C sample, sub-critical failure occurred at a low stress (~50 MPa): this was associated with fibrillation and debonding of the sample, while the samples made at 189 and 191 °C failed in a brittle manner. The stress–strain curves show that as the compaction temperature was increased, the post-yield modulus, which is a good indication of interlayer bonding, increased up to 189 °C. Typical measured values were 0.54, 0.58, 0.77 and 0.77 GPa, for the samples made at 179, 184.5, 187.5 and 189 °C: the post-yield modulus was measured between strains of 3 and 8%. Finally it is seen that the sample made at 191 °C showed behaviour similar to the melted film (Fig. 3, Polymer 2), indicating that too much melting of the original oriented structure had occurred at this temperature.

These results indicate that as the compaction temperature is increased, the percentage of melted material increases, thereby improving bonding (and stress transfer) and hence increasing modulus and strength. If too much melting occurs, a significant percentage of the oriented structure is lost and the modulus and strength decrease, although the bonding still continues to improve. These results suggest an 'optimum' compaction temperature of around 187.5 °C for cloth C. Interestingly, the results in Table 5 show a large difference in ultimate strength for a sample cut parallel to the weft and parallel to the warp directions.

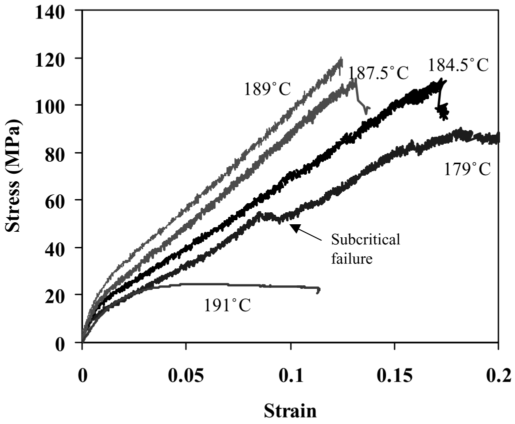

Fig. 4. Stress–strain behaviour of sheets of cloth C, compacted at 179, 184.5, 187.5, 189 and 191 °C, tested parallel to the weft direction.

Table 5
Mechanical properties of cloth C, compacted at a range of temperatures

| Compaction temperature (°C) | Initial tensile modulus (GPa) | | Ultimate tensile strength (MPa) | | Average peel load (N/10 mm) |
|---|---|---|---|---|---|
| | Weft | Warp | Weft | Warp | Parallel to weft |
| 179 | 2.3 | 1.7 | 55 | | 2.3 ± 0.4 |
| 182 | 2.2 | 1.9 | 55 | 50 | 2.8 ± 0.4 |
| 184.5 | 2.6 | 2.1 | 105 | 40 | 3 ± 0.5 |
| 185 | 2.8 | 2.6 | 140 | 62 | 3.8 ± 0.8 |
| 187.5 | 2.9 | 2.9 | 135 | 70 | 5.6 ± 0.6 |
| 189 | 2.9 | 2.9 | 120 | 64 | 7.2 ± 0.9 |
| 191 | 1.7 | 1.7 | 27 | 26 | Could not peel |

*E*, $\sigma$ ± 3%.

The optimum compaction temperature was next established for each cloth type: the properties of these optimum samples are shown in Table 6. For the reinforcements with a similar molecular weight (cloths C, D and E) the optimum compaction temperature was found to increase with the value of the initial modulus of the tapes, primarily related to the degree of molecular orientation: cloths D, E and C and polymers 3, 4 and 2 in ascending order. Table 7 shows a comparison of the density of the optimum compacted samples to that of the original oriented stock (polymer 3 was again too heavy to be measured in the density column). It is seen that there was a significant increase in the relative density, and hence the crystallinity, due to the compaction procedure. This has been seen before in a previous publication [19], and was described as 'significant reorganisation of the crystallisable portion of the structure'. Interestingly, the molecular weight after compaction was measured for one sample (cloth E, polymer 4) and was found to be unaffected by the compaction process, indicating that there is no chemical degradation caused by the compaction process. We can conclude that the principal effect of the compaction process is annealing and reorganisation of the crystalline portion.

Table 6
Mechanical properties of the 'optimum' compacted samples for each cloth style

| Cloth style | Compaction temperature (°C) | Tensile modulus (GPa) | | Tensile strength (MPa) | |
|---|---|---|---|---|---|
| | | Weft | Warp | Weft | Warp |
| A | 182 | 3.9 | 2.2 | 125 | 44 |
| B | 180 | 2.7 | 4.1 | 60 | 86 |
| C | 187.5 | 2.9 | 2.9 | 135 | 70 |
| D | 181 | 3.0 | 3.0 | 60 | 60 |
| E | 184 | 3.2 | 3.2 | 115 | 102 |

*E*, $\sigma$ ± 3%.

Table 7
Properties of the compacted materials

| Cloth numbers | Polymer code | | Density (kg/m$^3$) | $M_n$ | $M_w$ |
|---|---|---|---|---|---|
| A, B | 1 | Original fibres | 907 | – | – |
| | | Compacted sheet | 916 | – | – |
| C | 2 | Original fibrillated tape | 912 | – | – |
| | | Compacted sheet | 934 | – | – |
| E | 4 | Original tape | 910 | 78,100 | 360,000 |
| | | Compacted sheet | 934 | 79,900 | 346,000 |

DSC measurements on the optimum samples (Fig. 5) showed mostly similar melting endotherms, apart from compacted cloth D. All showed the appearance of a low temperature peak (∼165 °C), characteristic of the melted and recrystallised phase. Determination of the area of the higher peak (the remaining oriented phase) and that of the original fibres and tapes, allowed the percentage of the oriented phase lost (and therefore the amount melted phase produced) due to hot compaction, to be calculated for the five cloths. The percentage of oriented phase remaining was determined as 73, 66, 71, 78 and 68% for compacted cloths A, B, C, D and E, respectively. We can conclude that the amount of melted material required to obtain optimum compaction for the five cloths is similar, at ∼30%

Fig. 6 shows the stress–strain behaviour of the optimum compacted samples for the five cloths. Results are shown for samples cut parallel to both the weft and warp directions, and numerical values are given in Table 6.

Compacted cloth A showed very different properties in the two directions with the weft direction samples showing a much higher initial modulus, post-yield modulus and ultimate strength compared to the warp direction. This is probably a combination of two factors: firstly there are many more fibres in the weft direction (Fig. 1 and Table 1) and secondly, as we will see later, the bonding is poorer parallel to the warp direction.

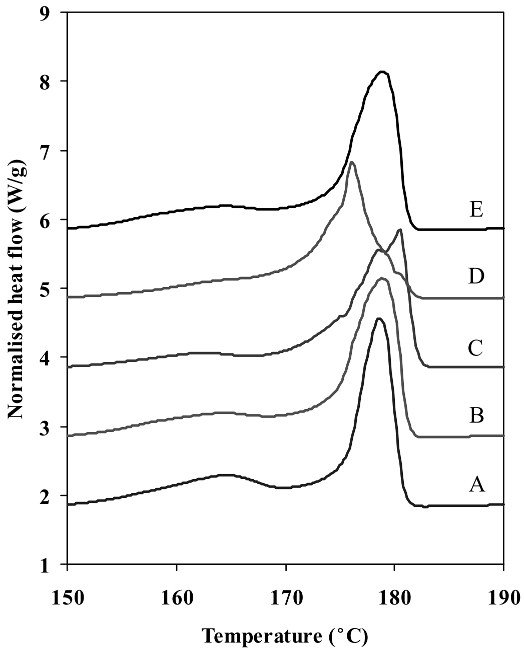

Fig. 5. DSC melting endotherms of the optimum samples for the five cloths A–E.

Compacted cloth B shows more balanced properties in the two directions, as a result of the number of fibres being more balanced in the warp and weft directions. However, the samples all failed by fibrillation and debonding, rather than across the section, suggesting poor bonding. As this cloth uses the same base polymer as cloth A then this poor bonding could be linked to the matrix properties, particularly the brittle nature seen at a similar cooling rate as shown in Fig. 3.

Compacted cloth C showed quite different properties in the two directions, which can be attributed to the weave style of the cloth. The degree of crimp in the warp direction was quite high, a consequence of quite a thick reinforcement.

Compacted cloths D and E, based on a flat tape reinforcement, and so with much less crimp in either the warp or the weft, showed more balanced properties between the warp and weft directions. Compacted cloth D showed lower tensile properties due, most likely, to the lower tensile properties of the original tape and also to the higher degree of crimp. Compacted cloth E (polymer 4) showed the best balance of properties of all five cloth styles, with a reasonable initial modulus, post-yield modulus and ultimate strength, in both the weft and warp directions.

### 3.3.2. Interlayer adhesion (peel strength)

Table 8 shows the average peel loads of the samples compacted at the optimum temperature, measured parallel to the weft and warp directions. Two conclusions are immediately clear from these results. Firstly, the compacted

Table 8
Peel strength of the optimum compacted samples

| Cloth style | Compaction temperature (°C) | Average peel load (N/10 mm) | |
|---|---|---|---|
| | | Parallel to weft | Parallel to warp |
| A | 182 | 1.7 ± 0.3 | 3.8 ± 0.5 |
| B | 180 | 2.0 ± 0.4 | 1.3 ± 0.2 |
| C | 187.5 | 6.4 ± 0.6 | 7.6 ± 1.8 |
| D | 181 | 12.2 ± 3.9 | |
| E | 184 | 6.3 ± 1.9 | 7.4 ± 2.3 |

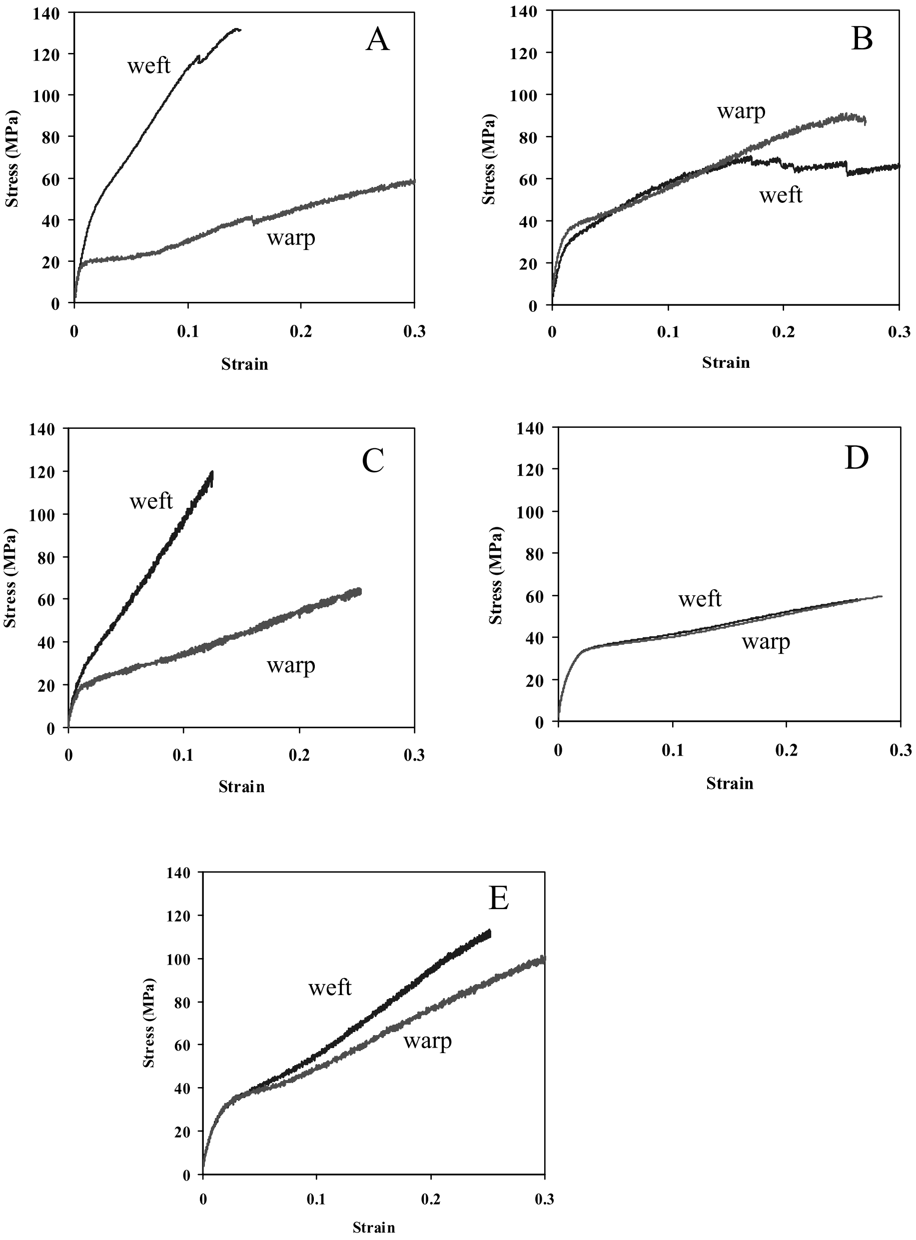

Fig. 6. Stress–strain curves for the optimum compacted samples for cloth A–E, for samples tested parallel to the weft and warp directions.

samples based on the lower molecular weight polymer, from cloths A and B, show lower average peel loads compared to those based on the more ductile, higher molecular weight, polymers (at least at the same cooling rate). Secondly, there are differences in the average peel load measured parallel to the weft and warp directions.

It is instructive to examine the actual peel load traces and the peel fracture surfaces. Fig. 7 shows peel load traces for compacted cloth A. For peeling parallel to the weft fibres (Fig. 7(a)), the peel load was fairly constant with occasional small peaks and troughs in the load. For peeling parallel to the warp (Fig. 7(b)), the trace was quite different. Here the average load was increased and the variation around the average load was much larger: the spacing between the peaks in the load was closer than for peeling parallel to the weft.

Fig. 8 shows low magnification stereomicroscope pictures of the fracture surfaces for this cloth, peeled parallel to the weft (8a) and parallel to the warp (8b). In order to show in an unbiased manner any differences in the appearance of the surface after peeling, the illumination was arranged to give both peel and perpendicular to peel directions equal prominence, as described in Section 2. Fig. 8 shows that there is a clear difference in the appearance of the fracture surfaces for peeling in the two directions. SEM micrographs taken at a higher magnification (Fig. 9(a) and (b), for peeling parallel to the weft and warp directions, respectively) confirm this difference in surface appearance with peeling direction. For peeling parallel to the weft, the fracture was parallel to the main crimp direction, while peeling parallel to the warp goes across the main crimp

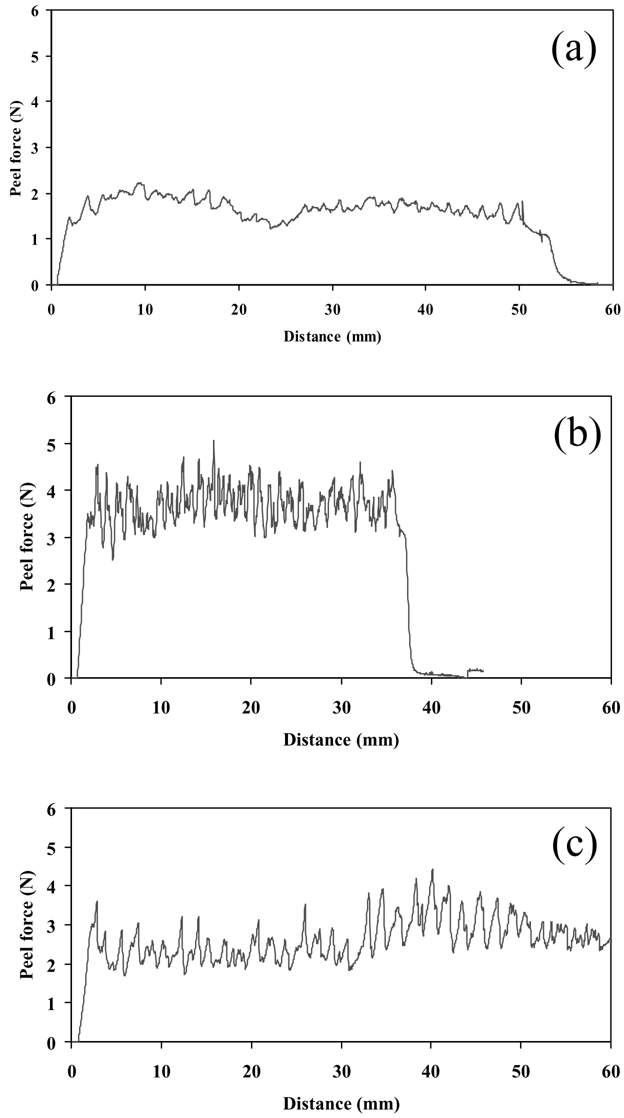

Fig. 7. Peel load traces for a compacted sample of cloth A: (a) peeled parallel to the weft direction, (b) peeled parallel to the warp direction) (c) 0/90 sample.

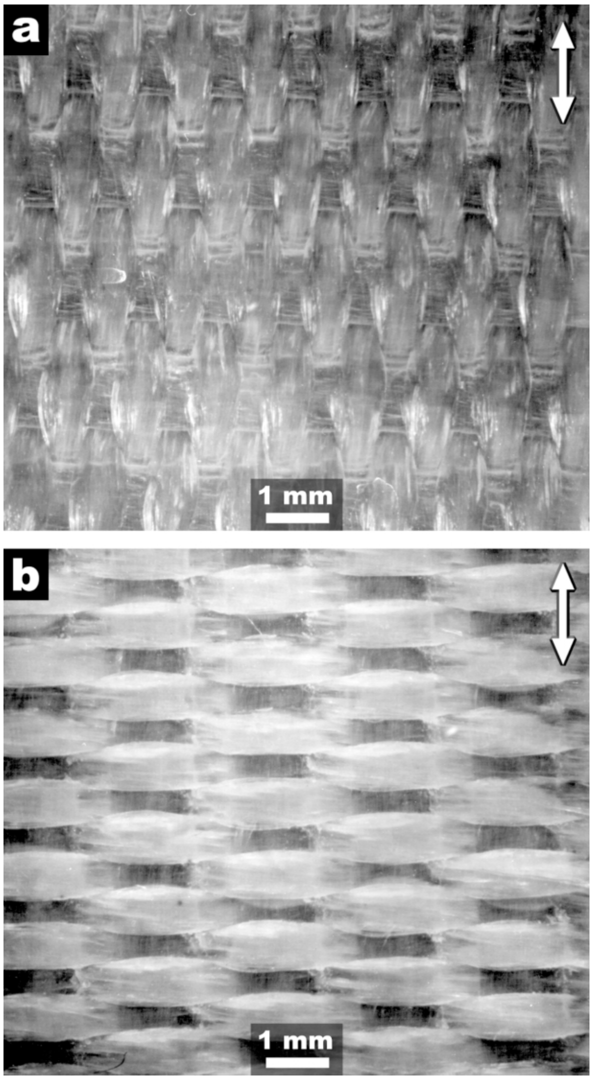

Fig. 8. Stereomicroscope peel fracture surfaces for cloth A: (a) peeled parallel to the weft, (b) peeled parallel to the warp. Arrows indicate peel direction.

direction. Referring back to Fig. 1, we remember that for this weave style there are more fibres in the weft direction than the warp direction. Therefore when peeling parallel to the warp direction, there are more fibre bundles which are transverse to the peeling direction, as shown by both Figs. 8 and 9. In fact we can go further, for the spacing of the load peaks in Fig. 7(b) is directly related to the distance between the weft fibre bundles. It is likely that peeling generates tensile stresses parallel to the peeling direction, which would tend to promote damage in fibre bundles transverse to the peeling direction, particularly as we have seen that the base polymer for this cloth style is very brittle, making it easy for damage to develop between the fibres.

There is, therefore, a clear geometry (or weave style) effect on the interlayer strength for compacted samples of cloth. A final experiment was carried out to confirm this effect, where two layers of cloth A were compacted together laid up in a 0/90 configuration, i.e. at 90° to each other. Fig. 7(c) shows the peel load trace for this experiment, and as expected, the peel load is mid way between the two previous results. The pitch of the load variation was also changed as might have been expected, to be a combination of the pitch for the 0/0 sample in the warp and weft directions.

The peel load for the other cloth based around the more brittle polymer 1, cloth B, was also low. Peel fracture surfaces for compacted samples of this cloth (Fig. 10), showed very little damage, or matrix ductility, on the surface. Even the bundles perpendicular to the peeling direction did not show significant damage, and this could be due to the much tighter weave style of this cloth (Fig. 1) limiting this potential damage mechanism. In an accompanying paper we will show that the matrix morphology also plays a key role in determining the interlayer peel strength.

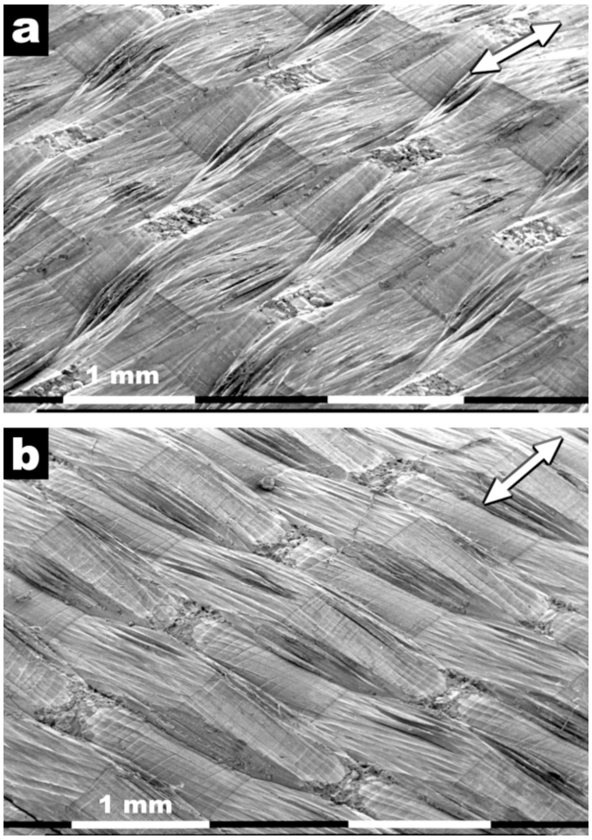

Fig. 9. SEM peel fracture surfaces for cloth A: (a) peeled parallel to the weft and (b) peeled parallel to the warp. Arrows indicate peel direction.

Next we consider the cloths based on the more ductile polymers. As stated above, all these showed much higher average peel loads (Table 8). Fig. 11 shows peel load traces for compacted samples of cloth C, peeled parallel to the weft (a) and warp (b) directions. Again there is a clear difference in the shape of these traces in the two directions, although the average load is not too different. Low magnification pictures of the fracture surfaces again confirm this difference in the appearance for peeling in the two directions. Fig. 12 shows stereomicroscope pictures of the two peeling directions, and Fig. 13 shows the corresponding SEM micrographs. The SEM pictures show a much higher level of damage than was seen on the fracture surfaces for cloths A and B, based on the more brittle polymer. There is a significant degree of tape splitting, in all cases parallel to the tape axis, or main orientation direction as would be expected. The SEM pictures suggest that damage is more evenly spaced this time between bundles that were parallel and transverse to the peeling direction, which is reflected in the more even parity of the average peel load in the two directions. There is still, however, a difference in the appearance of the two surfaces (Fig. 12) which is obviously due to differences in the weave structure. Stress–strain results for this cloth showed the weft direction to be much stiffer and stronger, and this was attributed to straighter fibres in the weft direction. These straight weft fibres form ridges on the cloth surface and when compacted together these can register and interlay. The ridges due to the straight weft fibres can be seen very clearly in Fig. 13(a) (indicated by the white arrowheads). Peeling perpendicular to this direction gave a very regular, oscillatory, peel load trace (Fig. 11(b) and at a higher scale in Fig. 11(c)), which is directly related to the weave spacing, with the spacing between the load peaks exactly half the weft spacing (a). Figs. 12(b) and 13(b), for peeling in this direction, show a regular banding structure across the peeled surfaces which is directly related to the spacing of the peaks in the load trace (Fig. 11(c)). This particular weave style showed this geometry effect more graphically than the other four cloths studied, for although it had a similar tape count to the other cloths, the reinforcement was thicker, which amplified the effect. It is worth noting, that while the average peel load for cloth C is similar for peeling in the two directions (Table 8), the peak values for propagating perpendicular to the weft are higher. It might be suggested that it is the peak values that are more important, as the load needs to be greater than the peak value for further propagation to occur. Another point worth noting is that it would be possible, by utilising straight fibres in one direction of a cloth, to promote better

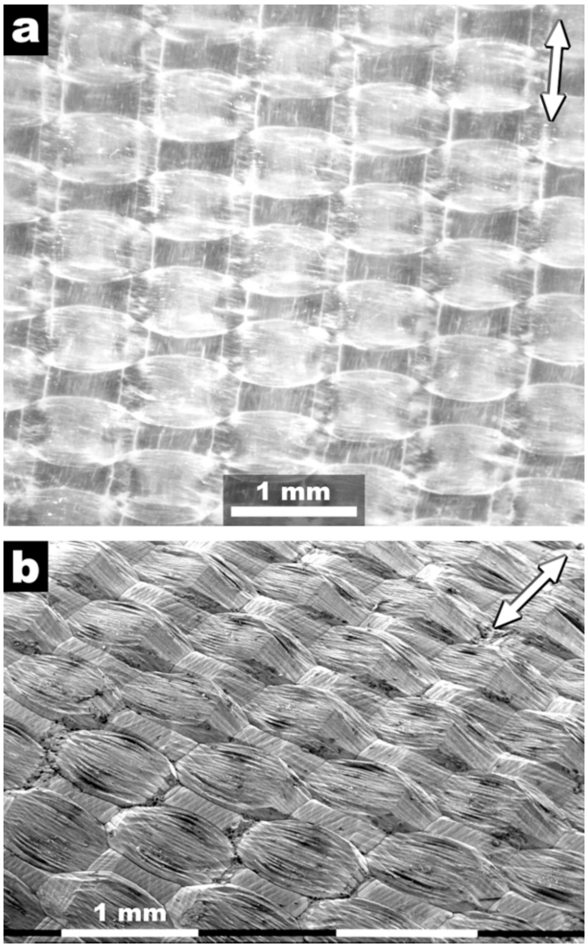

Fig. 10. Peel fracture surfaces for cloth B, peeled parallel to the weft: (a) stereomicroscope picture, (b) SEM picture. Arrows indicate peel direction.

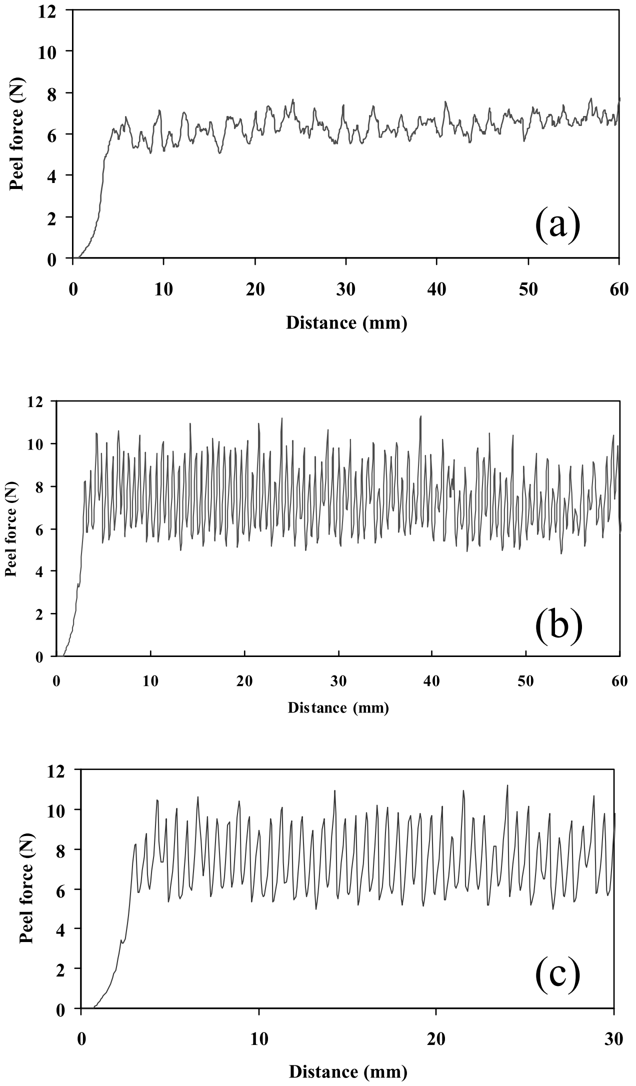

Fig. 11. Peel load traces for a compacted sample of cloth C: (a) peeled parallel to the weft, (b) peeled parallel to the warp, (c) expanded section of (b).

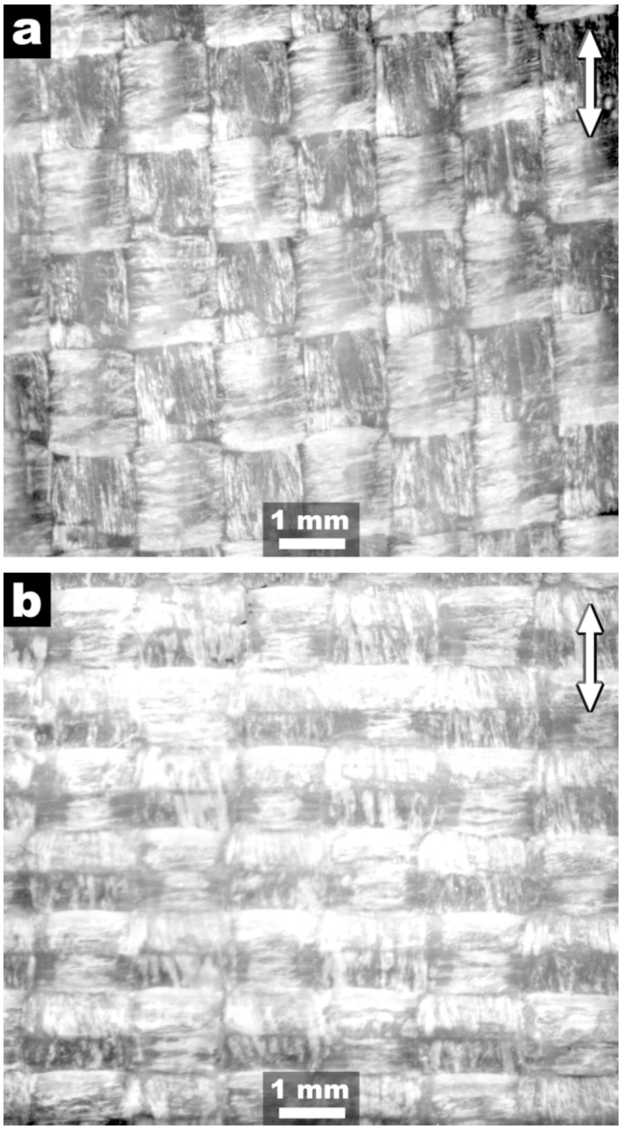

Fig. 12. Stereomicroscope peel fracture surfaces for cloth C: (a) peeled parallel to the warp and (b) peeled parallel to the weft. Arrows indicate peel direction.

bonding by interlocking. This, however, has the disadvantage that the in-plane modulus and strength values will then be different in the two directions, as seen with this cloth

Finally we consider the two weave styles based around the woven flat tapes, cloths D and E. In these materials, the peel strengths were also high. A typical load trace for a compacted sample from cloth E is shown in Fig. 14. The pitch of the load peaks is again close to that of the tape count, although this is more variable as the flat nature of the cloth surface does not favour any registering of the layers. Typical fracture surfaces for cloth E are shown in Fig. 15: Fig. 15(a) shows a stereomicroscope picture while Fig. 15(b) shows an SEM picture. As with cloth C, we can note how there is much more evidence of ductility on this fracture surface compared to those based on the brittle polymers. Because the reinforcing tapes are both thin and flat, and the weave style is balanced, the fracture surface looks similar for peeling in the two directions, and a similar peel load is seen in the two directions, this time for both the average and the peak values.

## 4. Discussion

The results presented above suggest strongly that we can consider a hot compacted polypropylene sheet as a composite, with an oriented polypropylene reinforcement bound together by an isotropic polypropylene matrix, As with all composites, the properties of the final material reflect the properties of the two component phases. Uniquely, in the hot compaction process, the matrix phase is formed by melting a proportion of the oriented phase. Therefore the fibre/matrix combination cannot be optimised as a normal

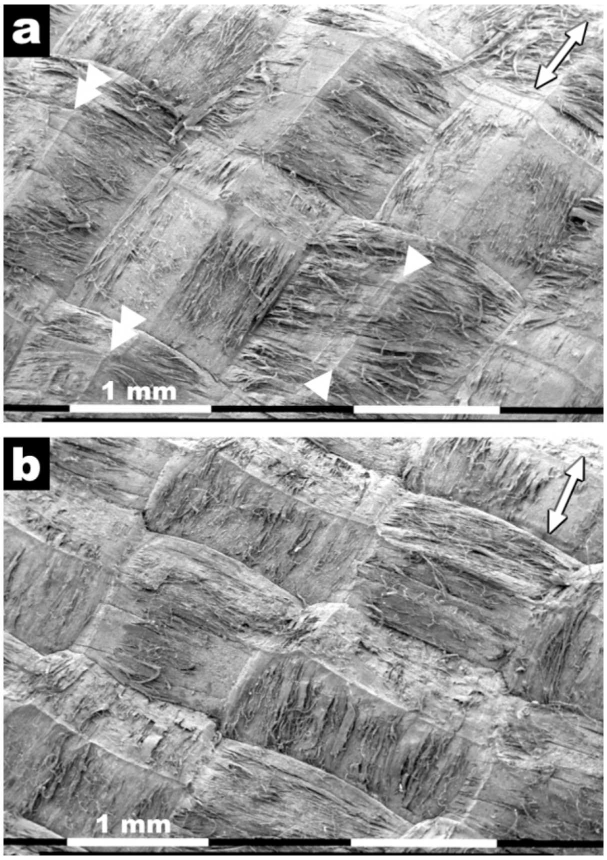

Fig. 13. SEM micrographs of cloth C peel fracture surfaces: (a) peeled parallel to the weft and (b) peeled parallel to the warp. Arrows at top right indicate peel direction.

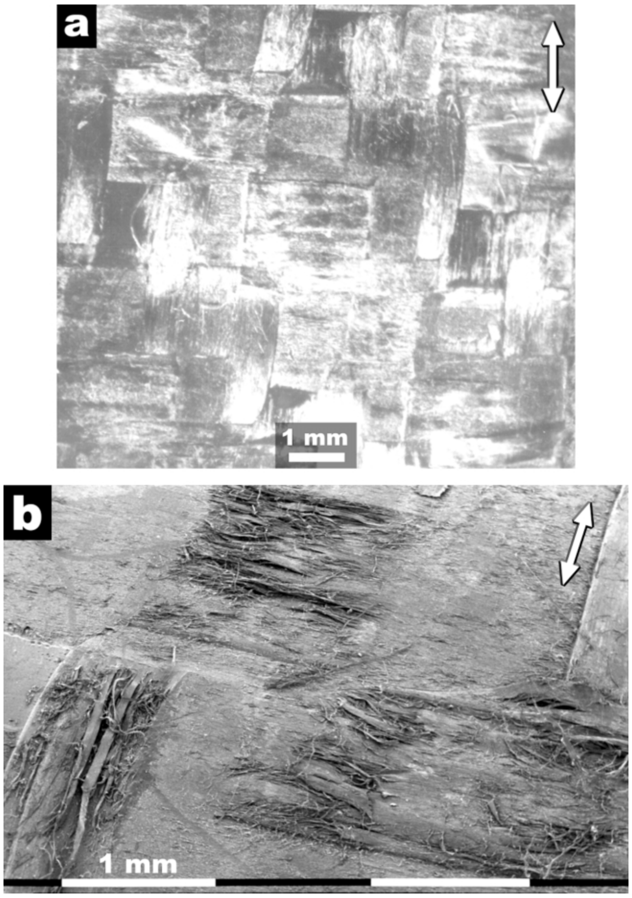

Fig. 15. Peel fracture surfaces for cloth E peeled parallel to the weft: (a) stereomicroscope picture, (b) SEM picture. Arrows indicate peel direction.

composite, where each phase is chosen on its merit. For a hot compacted composite, both phases are from the same source, and just because the oriented phase has a high modulus and strength, does not mean it will make a good matrix for the composite when melted (i.e. cloth A/Polymer 1).

Fig. 16 shows stress–strain curves for the original tape, melted matrix (with the appropriate cooling rate) and hot compacted composite for cloth E. As would be expected, the compacted composite properties lie between the properties of the fibre and matrix. While the DSC results shown in Fig. 5 suggest a 70% fraction for the oriented phase, the woven nature of the cloth results in a reduction in this percentage. The first effect of the weave style is that half the reinforcement will be perpendicular to any particular direction (either weft or warp) and as the transverse modulus of oriented polymers is very similar to the properties of the isotropic (or in our case the matrix phase) polymer this reduces the effective volume fraction by

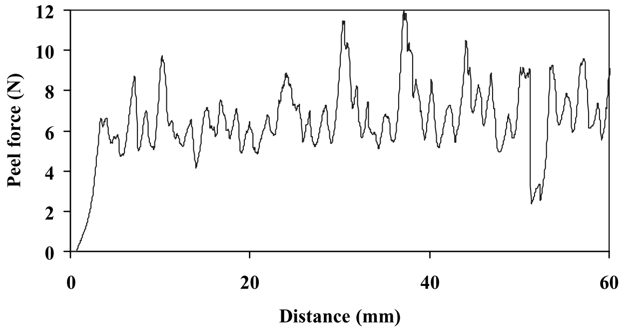

Fig. 14. Peel load traces for a compacted sample of cloth E: peeled parallel to the warp direction.

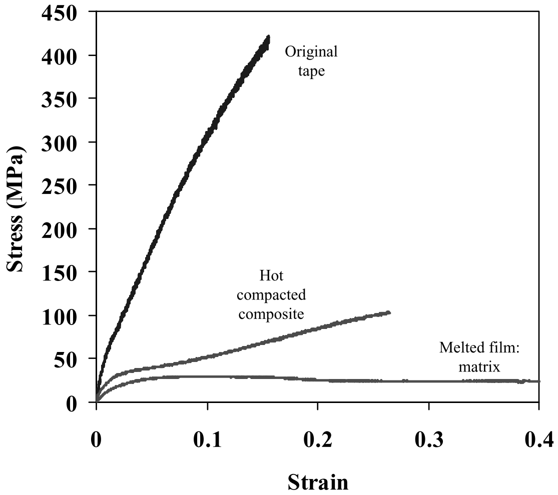

Fig. 16. A comparison of the stress–strain curves for the original tapes, the melted matrix film and the compacted composite for cloth E.

50%. Secondly the degree of crimp required by the weave style, will further reduce the effectiveness of the oriented phase.

It is possible to use standard composite models to predict the likely properties of the hot compacted PP composites. In particular, the parallel rule of mixtures for the composite Young's modulus $E_{\text{comp}}$, is given by

$$E_{\text{comp}} = E_{\text{tape}} V_{\text{tape}} + E_{\text{matrix}} V_{\text{matrix}} \tag{1}$$

where $V_{\text{tape}}$ and $V_{\text{matrix}}$ are the volume fraction of the reinforcing tape and matrix, respectively, and $E_{\text{tape}}$ and $E_{\text{matrix}}$ are the Young's moduli of the two phases. For the hot compacted composite shown in Fig. 15, this can be expressed as

$$E_{\text{comp}} = E_{\text{tape}} \frac{V_{\text{tape}}}{2} + E_{\text{matrix}} \left(1 - \frac{V_{\text{tape}}}{2}\right) \tag{2}$$

where $V_{\text{tape}}$ is the volume fraction of the oriented phase and $E_{\text{tape}}$ the Young's modulus of the original tape. Taking the results from Tables 2–4 gives $E_{\text{tape}} = 6.8$ GPa, $E_{\text{matrix}} = 1.22$ GPa and $V_{\text{tape}} = 0.7$. This would predict an upper limit for the hot compacted modulus, in the absence of fibre crimp, of 3.17 GPa. Considering the first order nature of this prediction, the agreement with the measured value from Table 6, of 3.2 GPa is excellent. Unknowns include any annealing effects on the oriented tapes due to the compaction procedure, whether the matrix recrystallises in a different manner in the presence of the oriented phase, and the exact calculation of the volume fraction of both phases from DSC measurements. The large increase in density, and hence inferred increase in crystallinity, seen in the compacted material, compared to the original tape, suggests there are significant structural changes occurring during the hot compaction procedure which have yet to be clarified.

So the initial modulus of the compacted sheets can be understood in terms of the properties of the two phases, the fraction of each and the weave style. The importance of the weave style, and the reinforcement shape, are shown by the results from the other cloths. If we take an average initial modulus from the five styles, to remove effects of different amounts of crimp/tape counts in the warp and weft directions, this gives values of 3.05, 3.5, 2.9, 3.0 and 3.0 for cloth A–E, respectively. Taking values for the original reinforcement from Table 2 gives the ratio of the compacted modulus to the original modulus for the five cloths, A–E as; 0.32, 0.37, 0.27, 0.47 and 0.44. Considering the fact that the matrix for cloth A and B has a higher modulus, the translation of the oriented reinforcement properties is probably even lower. It is seen that the thinner the reinforcement, the lower the degree of crimp and the better the translation of properties of the oriented phase to the compacted sheet. The thick fibrillated tapes of cloth C shows the lowest fraction, while the thin, flat tapes (cloths D and E) show the highest fraction.

This deals with the small strain behaviour of the compacted sheets. At higher strains the compacted sheets are seen to go through a yield point at around 2% strain (Fig. 16), which is clearly related to a similar yield point in the matrix behaviour. Past this strain, there is the possibility of the matrix failing, with the resulting poor stress transfer through the composite and an associated low post-yield modulus and ultimate strength. There is clearly a danger with the two cloths based around polymer 1 (cloths A and B), that its brittle nature, when cooled at the intermediate rate, could lead to premature failure. This behaviour, where the yield strain of the matrix is lower than that of the fibre, is quite unusual for a composite for it is normally the fibres which are stiff and inextensible and the matrix which is more ductile. In the case of hot compacted PP, this is a consequence of the well known effect of molecular orientation. The result is that it is obviously preferable to have a matrix, which remains ductile up to the point where the reinforcing phase fails. In this respect it is desirable to have a high molecular weight polymer.

The interlayer adhesion was found, as expected, to be primarily a matrix dependent property, although there are also obviously geometry effects due to the nature of the weave style. Flat tapes again appear a better style of reinforcement, as there was no preferred registering of the surfaces (as was seen when using thicker and straighter tape or fibre bundles) and so the peel strength was the same in both the weft and warp directions. Clearly the ductility of the matrix (through the molecular weight of the base polymer and the resulting differences in crystallinity) is also of prime importance, with more ductile polymers showing higher values of peel load. Cooling rate is also of importance, for the faster the cooling rate the lower the crystallinity and hence the more ductile the resulting matrix: the only drawback to this is a small reduction in the Young's modulus of the matrix phase.

In summary, it has been shown that the properties of a hot compacted polypropylene sheet can be understood in terms of the properties of the oriented phase, the melted and recrystallised phase and the weave style. It would appear that a high molecular weight for the base polymer is desirable because this leads to an increase in the ductility of the matrix. However, it is also well known that to obtain a highly oriented polypropylene tape or monofilament, a comparatively low value of $M_w$ is desirable [26]. It is likely that the five cloths chosen, relatively randomly, are not yet optimised for both fibre and matrix properties in terms of molecular weight. The results also show that the higher the modulus and strength of the original oriented phase, the higher the likely modulus and strength of the compacted sheets. Tape reinforcement appears better than multifilament bundles or fibrillated tapes because tapes can sit flatter in the cloth (less crimp), are more easy to weave into a balanced style and have less internal free space (less surface area). Finally a balanced weave style would appear to be best, unless a specific design requirement was required.

## 5. Conclusions

The major conclusion of this study is that hot compacted polypropylene sheet can be considered as a composite, with an oriented polypropylene reinforcement bound together by an isotropic polypropylene matrix. As with all composites, the properties of the final material depend on the properties of the two component phases. The role of the oriented reinforcing fibre or tape is to provide high stiffness and strength. It has been shown that simple rule of mixture ideas can be used to understand the properties of the compacted sheet in terms of the properties of the oriented reinforcement.

For the matrix phase, we have established the crucial importance of the level of ductility in controlling the properties of the hot compacted composite sheets. Unusually for a composite, the failure strain of the oriented reinforcement is higher than the melted and recrystallised matrix phase. It is therefore crucial to have as high a strain to failure for the matrix as possible, to allow the composite to retain its integrity up to the failure point of the reinforcement. Higher molecular weight and lower crystallinity (which was produced using a faster cooling rate) was found to improve ductility.

Finally clear geometry effects were seen, both in terms of the reinforcement shape and the weave style, which to some extent are interlinked. The best combination of properties was found for flat tapes, which gave less crimp when woven: a balanced weave style was also found to be beneficial.

## Acknowledgements

We are indebted to Mr Keith Norris for the meticulous sample preparation and engineering involved in this project. We would also like to thank Dr Steve Holding at RAPRA for carrying out the GPC measurements.

## References

[1] Ward IM. Adv Polym Sci 1985;70:1.

[2] Ward IM, Coates PD, Domoulin MM, editors. Solid phase processing of polymers. Munich: Hanser; 2000. Chapters 5 and 9.

[3] Capaccio G, Crompton TA, Ward IM. J Polym Sci, Polym Phys Ed 1976;14:1641.

[4] Taraiya AK, Richardson A, Ward IM. J Appl Polym Sci 1987;33:2559.

[5] Coates PD, Ward IM. J Polym Sci, Polym Phys Ed 1978;16:2031.

[6] Ladizesky NH, Ward IM. Compos Sci Technol 1986;26:129.

[7] Peijs T, Rijsdijk HA, Dekok JMM, Lemstra PJ. Compos Sci Technol 1994;52:449.

[8] Capiati NJ, Porter RS. J Mater Sci 1975;10:1671.

[9] Teishev A, Incardona S, Migliaresi C, Marom G. J Appl Polym Sci 1993;50:503.

[10] Marais C, Feillard P. Compos Sci Technol 1992;45:247.

[11] Hinrichsen G, Kreuzberger S, Pan Q, Rath M. Proceedings of the Ninth International Conference on the Mechanics of Composite Materials, Riga; October 1995.

[12] Lacroix Fv, Werwer M, Schulte K. Composites, Part A 1998;29A:371.

[13] Loos J, Schimansky T, Hofman J, Klompen E, Peijs T, Lemstra P. Proceedings of Euromat'99.

[14] Hine PJ, Ward IM, Olley RH, Bassett DC. J Mater Sci 1993;28:316.

[15] Olley RH, Bassett DC, Hine PJ, Ward IM. J Mater Sci 1993;28:1107.

[16] Kabeel MA, Olley RH, Bassett DC, Hine PJ, Ward IM. J Mater Sci 1994;29:4694.

[17] Rasburn J, Hine PJ, Ward IM, Olley RH, Bassett DC, Kabeel MA. J Mater Sci 1995;30:615.

[18] Yan RJ, Hine PJ, Ward IM, Olley RH, Bassett DC. J Mater Sci 1997;32:4821.

[19] Hine PJ, Ward IM, Teckoe J. J Mater Sci 1998;33:2725.

[20] Hine PJ, Bonner MJ, Brew B, Ward IM. Plast, Rubber Compos Process Appl 1998;27:167.

[21] Ward IM, Riley DE, Hine PJ, Brew B. Proceedings of the Automotive Composites Workshop, Brands Hatch; December 1998.

[22] Prosser W, Hine PJ, Ward IM. Plast, Rubber Compos 2000;29:401.

[23] Vincent PI. Encyclopedia Polym Sci Technol 1967;7:292.

[24] Stearne J, Ward IM. J Mater Sci 1969;4:1088.

[25] Brown N, Ward IM. J Mater Sci 1983;18:1405.

[26] Cansfield DLM, Capaccio G, Ward IM. Polym Engng Sci 1976;16:721.